BL12B2
NSRRC BM

BL12B2 is one of two contract beamlines operated by the National Synchrotron Radiation Research Center (NSRRC, Taiwan) in collaboration with the Japan Synchrotron Radiation Research Institute (JASRI) and RIKEN. Although originally designed for materials science and protein crystallography, the completion of the 3-GeV Taiwan Photon Source (TPS) at NSRRC has shifted the beamtime distribution. Over the past several years, most of the beamtime has been allocated to materials science users, approximately 75% of whom are from Taiwan. The remaining beamtime is shared among international users, including those from Japan and other countries.

Figure 1(a) schematically depicts the beamline layout. The beamline is equipped with a collimating mirror (CM), a double-crystal monochromator (DCM), and a focusing mirror (FM). The synchrotron beam was collimated with CM and monochromatized by DCM and focused to the experiment hutch(Fig.1(b)(c)). The measured spot size and total flux of the beam are about 250×250 μm and 1.5×10^{11} photons at the X-ray diffraction end-station at an incident photon energy of 12 keV, respectively. Three end-stations, projection X-ray microscopy (PXM), EXAFS, and powder X-ray diffraction (powder XRD), are positioned in tandem inside the experimental hutch of BL12B2.

The PXM end-station was installed in 2018. EXAFS experiments are performed at a dedicated table, and spectra can be measured in both transmission and reflection modes. High-pressure and powder X-ray diffraction (XRD) experiments are conducted at the protein crystallography table using a photon-counting CdTe detector. For temperature control, a nitrogen gas flow cryostat and a heat gun can vary the sample temperature from 60 to 500 K. A closed-cycle He cryostat is also available for lower temperature experiments. A plate-type diamond anvil cell (DAC) is used for high-pressure XRD. For in-situ electrochemical experiments, electrodes (AUTOLAB PGSTAT204,

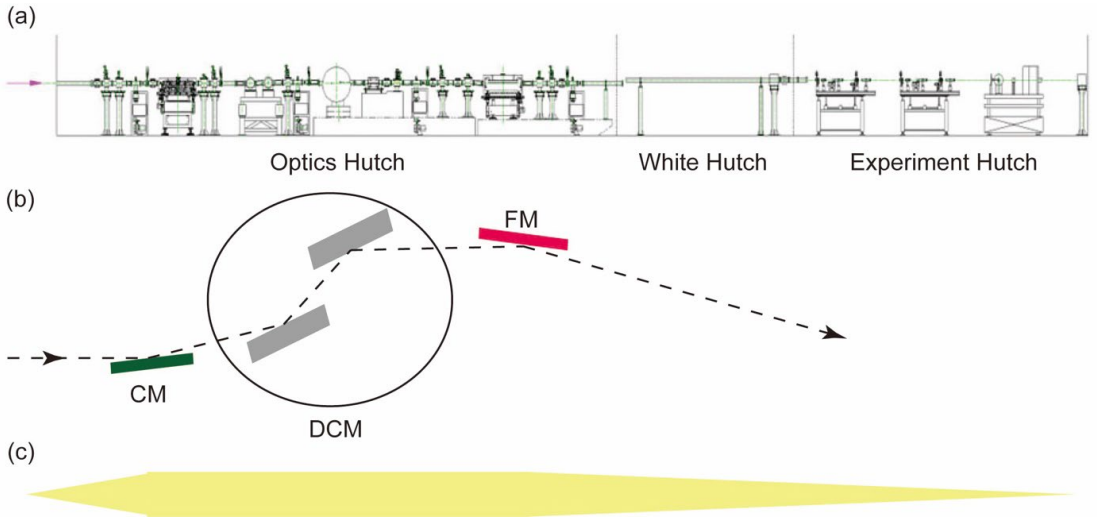

Fig. 1. (a) Schematic layout of BL12B2. (b) Side and (c) top views of beam trajectory.

Metrohm) have been prepared for both EXAFS and XRD. The beamline optics and end-station equipment are controlled by the software SPEC.

The Taiwan Beamline Upgrade Project began in early 2023. The project's goal is to upgrade existing beamline components to ensure their compatibility with the upcoming SPring-8-II. Each beamline component will be either replaced or maintained. In 2024, for example, we maintained DCM. We replaced the CCD detector for XRD with a photon-counting area detector, DECTRIS EIGER2 X CdTe 4M, in 2023 and commissioned it in 2024. The low noise and high count rate of this new detector will greatly benefit our XRD experiments. We plan to utilize this detector to expand our capabilities and begin conducting pair distribution function (PDF) experiments.

The BL12B2 beamline is dedicated to in situ and in operando X-ray experiments, with a primary focus on electrocatalysis. The aim of this research is to develop technologies like new energy materials, hydrogen production, and oxygen reduction, all of which are vital for a net-zero emission society [1–28]. The beamline is also utilized for studies on samples under extreme conditions, allowing us to investigate novel physical phenomena [29–37]. Figures 2 and 3 show selected recent results from a hydrogen generation study and a high-pressure XRD experiment on a giant dielectric sample, respectively. Figure 2 shows the results of a 3D TEM tomography and ex situ synchrotron XAFS study of RuNi nanoalloys supported on super-hydrophilic and high-curvature carbon (RuNi/NC) [19]. Figure 3 presents the results of research on the high-pressure XRD of $CaCu_3Ti_4O_{12}$ (CCTO), which exhibits a giant dielectric constant. They also studied the electronic structure of CCTO by X-ray Raman scattering experiment [33].

User support for BL12B2 is provided by two local beamline scientists and one engineer.

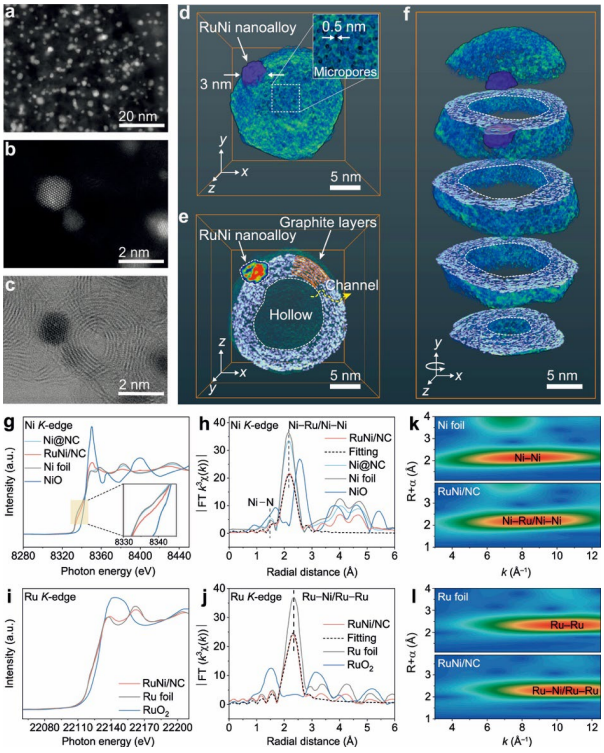

Fig. 2. (a)–(c) High-angle annular dark field (HAADF) and AC-STEM images of RuNi/NC. (d) 3D visualization of a single RuNi/NC nanoparticle, showing the partial embedding of RuNi nanoalloy within the carbon nanocage shell, achieved through an electron tomography technique. (e) Cross section of RuNi/NC, highlighting the multilayer porous shell and hollow cavity of the carbon nanocage. (f) Laminated cross sections and isosurfaces of RuNi/NC. (g) XANES and (h) Fourier-transformed (FT)-EXAFS spectra at the Ni K-edge of Ni@NC, RuNi/NC, Ni foil, and NiO. (i) XANES and (j) FT-EXAFS spectra at the Ru K-edge of RuNi/NC, Ru foil, and RuO_2.

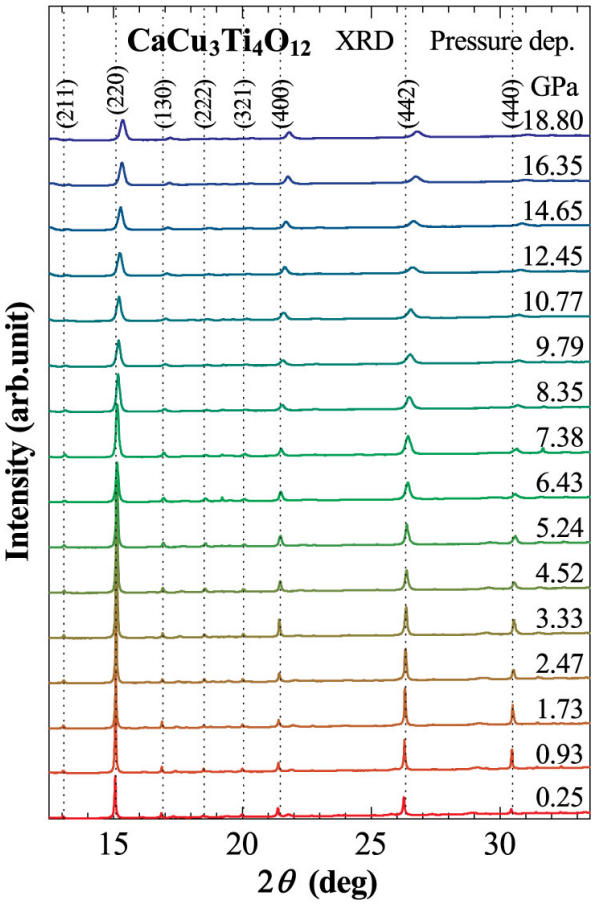

Fig. 3. Pressure-dependent X-ray diffraction patterns of CCTO. Values next to each pattern denote the pressure in GPa [33].

ISHII Hirofumi, SHAO Yu-Cheng, YOSHIMURA Masato, TATSUMI Tatsuya, and HIRAOKA Nozomu

National Synchrotron Radiation Research Center, Hsinchu 300092, Taiwan

References:

[1] Chiniwar, S. P. et al. (2024). *ACS Appl. Electron. Mater.* **6**, 1078.

[2] Yang, W. T. et al. (2024). *Appl. Catal. B-Environ.* **352**, 124017.

[3] Wang, M. et al. (2024). *Adv. Funct. Mater.* **34**, 2309474.

[4] Chu, Y. C. et al. (2024). *Adv. Mater.* **36**, 2400640.

[5] Wang, M. et al. (2024). *Chem. Eng. J.* **479**, 147505.

[6] Tu, T. C. et al. (2024). *Chem. Eng. J.* **487**, 150623.

[7] Faceira, B. et al. (2024). *ACS Appl. Energy Mater.* **7**, 9882.

[8] Xu. X. et al. (2024). *ACS Catalysis* **14**, 12051.

[9] Zhao, Y. et al. (2024). *Adv. Mater.* **36**, 2308243.

[10] Bhalothaia, D. et al. (2024). *Chem. Eng. J.* **483**, 149421.

[11] Ma, J. J. et al. (2024). *Electrochim. Acta.* **500**, 144744.

[12] Zhan, G. et al. (2024). *J. Am. Chem. Soc.* **146**, 16659.

[13] Chen, H. C. et al. (2024). *J. Environ. Chem. Eng.* **12**, 111741.

[14] Lin, T. Y. et al. (2024). *J. Mater. Chem. A* **12**, 7536.

[15] Zeng, W. J. et al. (2024). *Mater. Today Sustain.* **27**, 100820.

[16] Liao, F. H. et .al. (2024). *Nano Lett.* **24**, 11202.

[17] Zhang, P. et al. (2024). *Nat. Commun.* **15**, 2062.

[18] Zhao, S. et al. (2024). *Nat. Commun.* **15**, 2728.

[19] Zhang, L. et al. (2024). *Nat. Commun.* **15**, 7179.

[20] Cai. Y. M. et al. (2024). *Rare Metals* **43**, 5792.

[21] Wang, J. et al. (2024). *Angew. Chem. Int. Edit.* **63**, e29249333.

[22] Li, R. et al. (2024). *J. Colloid Interf. Sci.* **674**, 326.

[23] Xu, X. et al. (2024). *Adv. Funct. Mater.* **34**, 2408823.

[24] Sun, H. et al. (2024). *Adv. Funct. Mater.* **34**, 2408872.

[25] Chen, D. et al. (2024). *Adv. Mater.* **36**, 2410537.
[26] Zhang, J. et al. (2024). *Angew. Chem. Int. Edit.* **63**, e202412245.
[27] Deng, L. et al. (2024). *J. Am. Chem. Soc.* **146**, 23146.
[28] Deng, L. et al. (2024). *J. Am. Chem. Soc.* **146**, 35438.
[29] Yamaoka, H. et al. (2024). *Phys. Rev. B* **110**, 205129.
[30] Vrankić, M. et al. (2024). *Inorg.* **12**, 99.
[31] Eguchi, R. et al. (2024). *Inorg. Chem.* **63**, 947.
[32] Zhang, Z. et al. (2024). *Inorg. Chem.* **63**, 2553.
[33] Tezuka, Y. et al. (2024). *Phys. Rev. B* **109**, 35132.
[34] Yamaoka, H. et al. (2024). *Phys. Rev. B* **109**, 155147.
[35] Zhang, Z. et al. (2024). *Inorg. Chem.* **63**, 21531.
[36] Ishiwata, Y. et al. (2024). *J. Phys. Soc. Jpn.* **93**, 44603.
[37] Happo, N. et al. (2024). *Chem. Mater.* **36**, 4135.